SUPPLEMENTARY DATA

Supplementary Material A. Differences Between Look AHEAD Participants at the Three MRI Clinical Site Who Underwent MRI And Are Included in the Analysis Versus Those Who Are Not Included In Analysis

At the three sites, 321 (37%) individuals agreed to participate, were eligible for the study, and completed the MRI; 319 (99%) images met quality control standards and form the basis of this paper.Compared to the remaining 554 of the 875 potential recruits (i.e. active Look AHEAD participants at these sites who did not undergo MRI), based on t-tests (mean $\pm$ standard deviation) and chi-squared tests, the MRI sample was slightly younger (58.0±6.5 vs 59.3±6.8 years, p=0.005), had lower BMI (35.6±5.6 vs. 36.7±5.9 kg/m^2, p=0.007), had greater baseline cardiorespiratory fitness (7.3±2.0 vs 7.0±2.0 METS, p=0.03), was more likely to be female (70.2% vs. 56.5%, p<0.0001), and was less likely to be white (73.0% vs 82.0%, p=0.007).

SUPPLEMENTARY DATA

Supplementary Material B. MRI Methods Description

Image acquisition

All imaging was performed in the sagittal plane using parallel imaging with an acceleration factor of 2 and a 12 channel head coil.High-resolution (0.98 mm x 0.98 mm x 1 mm) T1-weighted structural scans used a 3D MPRAGE sequence (acquisition time = 4:26, TR = 1.9 seconds, TE = 2.89 ms, FOV 250 mm, matrix size 256 x 256, 176 slices).The 3D FLAIR sequence had an image resolution of 0.97 x 1.13 x 1mm (acquisition time = 8:20, TR = 6 seconds, TI = 2.2 seconds, TE = 160 ms, FOV 250 mm, matrix size 258 x 221, 160 slices).The T2-weighted images had a resolution of 0.97 x 0.98x 1mm (acquisition time = 4:08, TR = 3.2 seconds, TE = 409 ms, FOV 250 mm, matrix size 258 x 256, 176 slices).

Multi-atlas ROI segmentation

The image-analysis used an automated computer program to classify supratentorial brain tissue into either normal or abnormal gray or white matter and assign the tissue type to each of 154 anatomic regions of interest (ROIs) of the cerebrum.T1-weighted volumetric MRI scans were first pre-processed according to a standardized protocol for removal of extra-cerebral tissue, using an in-house method (S6).The brain was segmented into gray matter, white matter, and cerebrospinal fluid using MICO, a method proposed for joint bias field estimation and tissue segmentation (S7).

An ROI segmentation method (S8), based on multi-atlas registration using DRAMMS (S9) and label fusion, was used then to derive regional volumetric measurements.In this framework, semi-automatically extracted reference ROI labels from multiple atlases are warped individually to the target image and are fused together to assign a label to each voxel of the target image.The proposed method (S2) uses a consensus labeling framework, by generating a broad ensemble of labeled atlases via the use of two different non-linear image registration algorithms, followed by a spatially adaptive weighted voting strategy to fuse the ensemble into a final segmentation. In the fusion, a local similarity term is used for ranking and weighting reference labels from different atlases, and an image intensity based term is used for modulating the segmentations in the boundaries of the ROIs according to the intensity profile of the subject image.Portrayed in the figure is example segmentation.The method partitioned the T1 image into 154 anatomical regions, which were organized within a hierarchical structure to allow derivation of volumetric measurements in various resolution levels.These ROIs, organized in an anatomically hierarchal system, were then collapsed into the four anatomic ROIs used in the analysis we report (gray matter, white matter, ventricles, and hippocampus).

SUPPLEMENTARY DATA

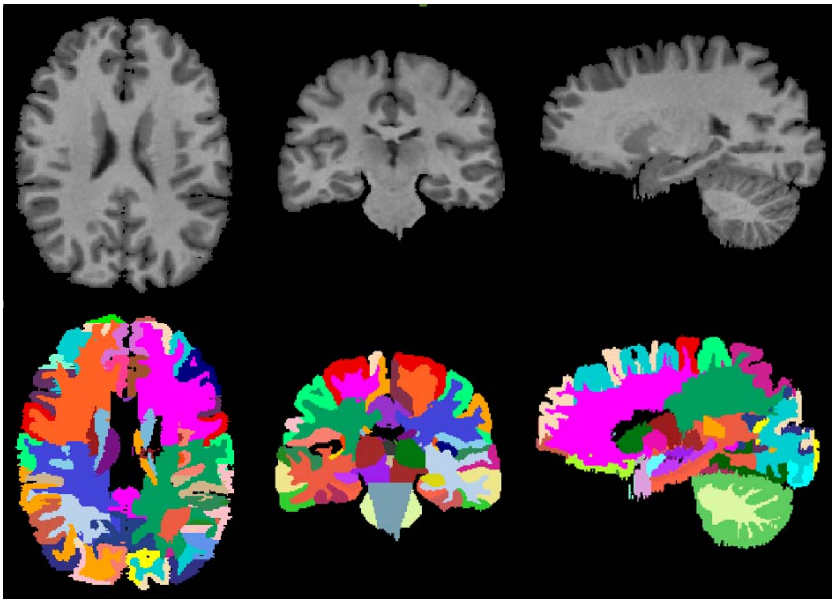

White matter hyperintensity segmentation

White matter hyperintensities were segmented using a multimodal segmentation technique, WMLS (S3), which was previously applied in a number of studies of similar nature (S4-S5). WMLS is a supervised learning method that trains on hyperintensities manually delineated by an expert radiologist.The hyperintensity segmentation involves data preprocessing via histogram standardization and co-registration, feature extraction from multi-modal MR scans, training a voxel-wise discriminative model using a support vector machine classifier, voxel-wise label assignment using the trained model and false-positive elimination.Multi-parametric MRI sequences (i.e., T1, T2 and FLAIR) from each participant were first co-registered and intensity normalized.White matter voxels were then classified as either hyperintensities or normal according to the training model.

White matter hyperintensity volumes correspond to what has been called leukoaraiosis, ischemic white matter disease, and/or small vessel ischemia.This process is now accepted as a non-necrotic, ischemic effect on myelin that is secondary to the effects of aging, hypertension, and other small vessel pathologic processes of the brain.The quantitative computerized digital image analytical techniques that these studies have employed are reproducible and offer great dynamic range.We used automated computer analysis for segmentation of these white matter hyperintensities, which were then assigned to anatomical regions according to the aforementioned parcellation scheme.

SUPPLEMENTARY DATA

Supplementary Material C. Median Percent Weight Changes From Baseline For Annual Visits Occurring Prior to Date of MRI

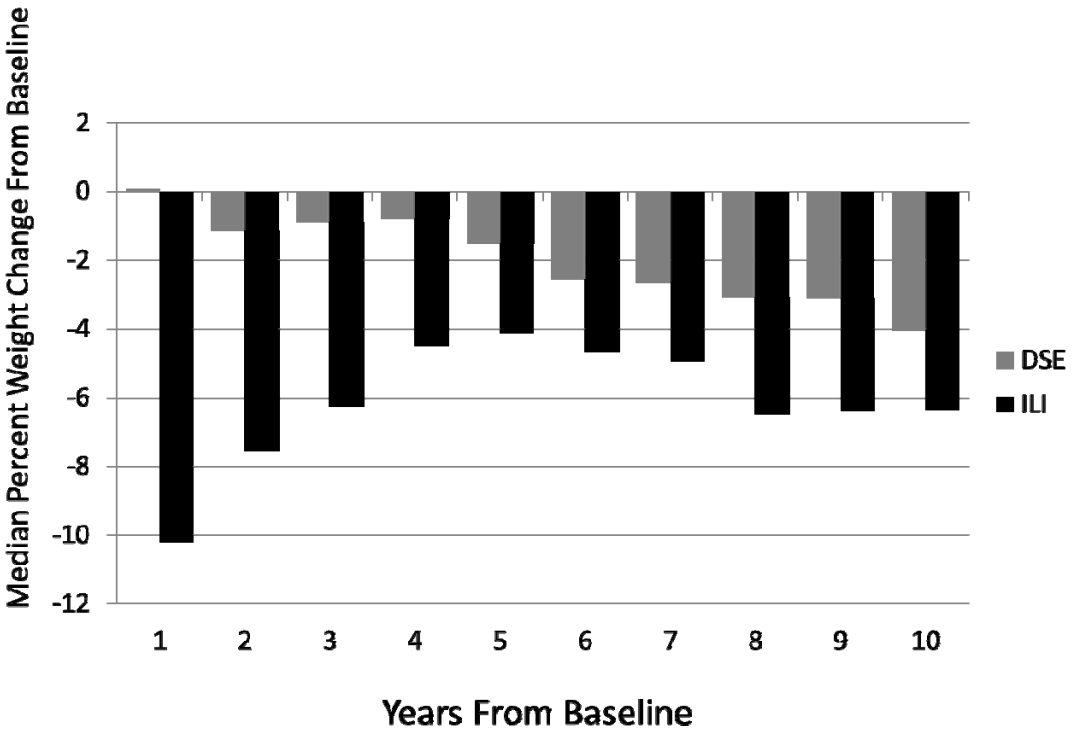

References

S1. Iglesias JE, Sabuncu MR. Multi-atlas segmentation of biomedical images: A survey. Medical Image Analysis 2015;24(1):205-219.

S2. Doshi J, Erus G, Ou Y, et al. MUSE: MUlti-atlas region Segmentation utilizing Ensembles of registration algorithms and parameters, and locally optimal atlas selection. Neuroimage 2015 DOI: 10.1016/j.neuroimage.2015.11.073

S3. Lao Z, Shen D, Liu D, et al. Computer-assisted segmentation of white matter lesions in 3D MR images using support vector machine. Acad Radiol 2008;15:300-313.

S4. Coker LH, Hogan PE, Bryan NR, et al. Postmenopausal hormone therapy and subclinical cerebrovascular disease: The WHIMS-MRI Study. Neurology 2009;72:125–134.

S5. Launer LJ, Miller ME, Williamson JD, et al. Effects of intensive glucose lowering on brain structure and function in people with type 2 diabetes (ACCORD MIND): a randomised open-label substudy. Lancet Neurol 2011;10:969–977.

S6. Doshi J, Erus G, Ou Y, Gaonkar B, Davatzikos C. Multi-atlas skull-stripping, MASS. Acad Radiol 2013;20:1566-1576.

SUPPLEMENTARY DATA

S7. Li C, Gatenby C, Wang L, Gore JC. A robust parametric method for bias field estimation and segmentation of MR images. Comp Vision Pattern Recog 2009. IEE DOI: 10.1109/CVPR.2009.5206553

S8. Ou Y, Sotiras A, Paragios N, Davatzikos C. DRAMMS: Deformable registration via attribute matching and mutual-saliency weighting. Med Image Analysis 2011;15(4):622-639.

S9. Ou Y, Doshi J, Erus G, Davatzikos D. Attribute similarity and mutual-saliency weighting for registration and label fusion. MICCAI Workshop on Multi-Atlas Segmentation. 2012; pp. 95-98.